



OPEN ACCESS

EDITED BY
Zhen Luo,
Jinan University, China

REVIEWED BY
Deyan Chen,
Nanjing University, China
Yang Qingyu,
Wuhan Jinyintan Hospital, China
Tong Cheng,
Xiamen University, China

*CORRESPONDENCE
Wei Wei
✉ wwei6@jlu.edu.cn
Haoran Guo
✉ sheng315640@163.com

SPECIALTY SECTION
This article was submitted to
Viral Immunology,
a section of the journal
Frontiers in Immunology

RECEIVED 08 December 2022
ACCEPTED 24 January 2023
PUBLISHED 09 February 2023

CITATION
Yang Q, Li H, Li Z, Yang J, Zhang Z,
Zhang L, Guo H and Wei W (2023)
Pterostilbene, an active constituent
of blueberries, enhances innate
immune activation and restricts
enterovirus D68 infection.
Front. Immunol. 14:1118933.
doi: 10.3389/fimmu.2023.1118933

COPYRIGHT
© 2023 Yang, Li, Li, Yang, Zhang, Zhang,
Guo and Wei. This is an open-access article
distributed under the terms of the [Creative
Commons Attribution License \(CC BY\)](#). The
use, distribution or reproduction in other
forums is permitted, provided the original
author(s) and the copyright owner(s) are
credited and that the original publication in
this journal is cited, in accordance with
accepted academic practice. No use,
distribution or reproduction is permitted
which does not comply with these terms.

Pterostilbene, an active constituent of blueberries, enhances innate immune activation and restricts enterovirus D68 infection

Qingran Yang¹, Huili Li¹, Zhaoxue Li¹, Jiaxin Yang¹, Zhe Zhang¹,
Lili Zhang¹, Haoran Guo^{1*} and Wei Wei^{1,2*}

¹Key Laboratory of Organ Regeneration and Transplantation of Ministry of Education, Institute of Translational Medicine, First Hospital, Jilin University, Changchun, Jilin, China, ²Institute of Virology and Acquired Immune Deficiency Syndrome (AIDS) Research, First Hospital, Jilin University, Changchun, Jilin, China

Enterovirus D68 (EV-D68) is a globally re-emerging respiratory pathogen implicated in outbreaks of severe respiratory illnesses and associated with acute flaccid myelitis. However, effective vaccines or treatments for EV-D68 infections remain scarce. We demonstrated that the active constituent of blueberries, pterostilbene (Pte), and its major metabolite, pinostilbene (Pin), facilitated innate immune responses in EV-D68-infected human respiratory cells. Pte and Pin treatment clearly relieved EV-D68-triggered cytopathic effects. Importantly, both Pte and Pin disrupted viral RNA replication (EC_{50} rank from 1.336 to 4.997 μ M) and infectious virion production in a dose-dependent manner, without cytotoxicity at virucidal concentrations. Pte- or Pin-treated respiratory cells did not show any influences on EV-D68 entry but showed substantially decreased viral RNA replication and protein synthesis. Finally, we showed that Pte and Pin broadly suppressed the replication capacity of circulating EV-D68 strains isolated from recent pandemics. In summary, our results suggest that Pte and its derivative, Pin, enhance host immune recognition of EV-D68 and suppress EV-D68 replication, which represents a promising strategy for antiviral drug development.

KEYWORDS

EV-D68, pterostilbene, pinostilbene, interferon, innate immunity, antivirals

1 Introduction

Enterovirus D68 (EV-D68), a member of the genus *Enterovirus*, belongs to the family *Picornaviridae* (1). EV-D68 contains a single positive-stranded RNA genome that includes an open reading frame (ORF). The ORF encodes the viral polyprotein, which can be digested by viral proteases to generate structural proteins (VP1–4) and non-structural proteins (2A–C and 3A–D) (2). The EV-D68 particle consists of 60 copies of each of the subunit proteins,

VP1, VP2, VP3, and VP4. Each of the 12 pentameric vertices circles a deep surface depression, which contributes to receptor binding (3). Previous studies have found that sialic acid on the host cytomembrane facilitates EV-D68 infection (4). Human intercellular adhesion molecule 5 has been identified as a virus receptor for sialic acid-dependent and -independent EV-D68 viruses (5).

Contrary to the majority of enteroviruses transmitted *via* the 'fecal-oral' route, EV-D68 is a respiratory virus, and its infection can cause acute respiratory symptoms. EV-D68 is more sensitive to low pH and prefers cold conditions (6). Recently, accumulating evidence has suggested that EV-D68 infection is associated with clusters of acute flaccid myelitis (7). EV-D68 was considered a rare virus for a long time after its initial identification in 1962 (8), until its largest outbreak in North America in 2014 (9). The prevalence of this virus has been increasing in recent years, although an effective anti-EV-D68 treatment remains unavailable. Therefore, there is an urgent need for antiviral agents to control EV-D68 infection and transmission.

Pterostilbene (Pte), a naturally abundant compound in blueberries, is a methoxylated analog of resveratrol (10). Pte has been extensively investigated because of its therapeutic advantages in decreasing insulin resistance; controlling glucose and lipid levels; relieving cardiovascular diseases, inflammatory diseases, and aging; and improving memory and cognition (11). Pte treatment facilitates apoptosis, cell cycle arrest, DNA damage, and overloaded autophagy in carcinoma cells without affecting normal cells, making it an ideal anti-tumor agent (12). However, whether Pte can serve as an antiviral drug against EV-D68 replication remains unknown.

Here, we demonstrated that treatment with Pte or its major metabolite, pinostilbene (Pin), activated host antiviral immunity in the presence of EV-D68 infection. This finding prompted us to investigate the effects of Pte and Pin on EV-D68 infection in human respiratory cells. The tested small-molecule inhibitors dramatically interfered with EV-D68-mediated cytotoxicity and suppressed viral RNA replication, protein synthesis, and infectious viral particle production. Therefore, our results demonstrate that Pte and Pin have potential clinical value in anti-EV-D68 therapy.

2 Materials and methods

2.1 Cells, virus, and reagents

A549 human lung adenocarcinoma cells (CCL-185, ATCC), human rhabdomyosarcoma (RD) cells (CCL-136, ATCC), and BEAS-2B human bronchial epithelial cells (CRL-9609, ATCC) were maintained in Dulbecco's Modified Eagle medium (DMEM; Sigma-Aldrich, USA), supplemented with 10% fetal bovine serum (FBS; Biological Industries, USA) and 1% penicillin/streptomycin. All cells were cultured at 37°C and 5% CO₂.

EV-D68 prototype Fermon (VR-1826, ATCC), isolated in California in 1962, and isolated EV-D68 circulating strains from the 2014 United States outbreak, US/MO/14-18947 (VR-1823D, ATCC) and US/KY/14-18953 (VR-1825D, ATCC), were propagated in RD cells at 37 °C, and stored at -80 °C. Viruses in the supernatants of infected cells were harvested three days post-infection following three freeze-thaw cycles. Samples were clarified by low-speed

centrifugation and then passed through a 0.22 μm filter. Viral particles were pelleted using 20% sucrose and centrifuged at 28,000 rpm using an SW28 rotor for 120 min (Beckman). Purified virions were stored at -80 °C.

Pterostilbene (HY-N0828, 99.83% purity) and pinostilbene (HY-N3059, 98% purity) were purchased from MedChemExpress (Monmouth Junction, NJ, USA).

2.2 Cell viability assay

Approximately 1.6×10^4 A549 or BEAS-2B cells per well were seeded into 96-well plates with complete media and incubated at 37 °C with 5% CO₂. When the cells were 90% confluent, the cell culture medium was removed and replaced with dimethyl sulfoxide (DMSO) or dose-gradient pterostilbene/pinostilbene. Cells were incubated for 24 h, and then 10 μL of Cell Counting Kit-8 reagent (CCK-8; MCE, Cat No.: HY-K0301) was added to each well. Absorbance was detected after 30 min using a BioTek plate reader (BioTek Instruments, Inc., USA) at a wavelength of 450 nm. Each data point represents the average of three technical replicates. 50% cytotoxicity concentrations (CC₅₀) of pterostilbene or pinostilbene were calculated.

2.3 RNA quantification using qRT-PCR

Total RNA was isolated from cells using TRIzol (Life Technologies) according to the manufacturer's instructions and included the DNase I digestion step. RNA was then converted to cDNA using a reverse transcription kit (Transgen Biotech, Beijing, China). PCR amplification was carried out on a LightCycler 480 Instrument II (Roche, Basel, Switzerland) with SYBR Green Supermix (Monad Biotech Co., Ltd., Wuhan, China). PCR cycling conditions used were: 95 °C for 2 min, followed by 40 cycles of 95 °C for 30 s and 60 °C for 1 min, with a final dissociation step of 95 °C for 5 min. Single peaks in the melting curve analysis indicated specific amplicons. The qRT-PCR was performed using the following primer sequences: glyceraldehyde-3-phosphate dehydrogenase (GAPDH) forward primer, 5'-GCAAATTCATGGCACCCT-3'; GAPDH reverse primer, 5'-TCGCCCCACTTGATTTTGG-3'; EV-D68 forward primer, 5'-TGTTCACGGTTGAAAACAA-3'; EV-D68 reverse primer, 5'-TGTCTAGCGTCTCATGGTTTTTTCAC-3'; interferon (IFN)-β forward primer, 5'-TTGTGCTTCTCCACTACAGC-3'; IFN-β reverse primer, 5'-CTGTAAGTCTGTTAATGAAG-3'; interferon-induced protein with tetratricopeptide repeats 1 (IFIT1) forward primer, 5'-CAACCAAGCAAATGTGAGGA-3'; IFIT1 reverse primer, 5'-AGGGGAAGCAAAGAAAATGG-3'; MX dynamin-like GTPase 1 (MX1) forward primer, 5'-GTTTCCGAAGTGGACATCGCA-3'; and MX1 reverse primer, 5'-CTGCACAGGTTGTTCTCAGC-3'. The relative levels of EV-D68 RNA in different samples were determined using the comparative $2^{-\Delta\Delta CT}$ method with normalization against the GAPDH gene (5).

2.4 Viral attachment assay

Cells were washed with cold (4 °C) or pre-warmed (37 °C) phosphate-buffered saline (PBS), and then incubated with EV-D68

(multiplicity of infection, MOI = 1). After incubation at 4 °C or 37 °C for 2 h, cells were washed with cold or pre-warmed PBS to remove unbound viruses. Total RNA was extracted and relative viral RNA level was determined using qRT-PCR, as mentioned above.

2.5 Virus titer assay

Viral titers were determined using an endpoint dilution assay (EPDA). Briefly, RD cells were cultured under standard conditions in 96-well plates at a density of 10,000 cells/well. EV-D68 was serially diluted (10-fold) in DMEM containing 1% FBS and added to the cells. Viral titers were determined by the appearance of cytopathic effects (CPEs) in RD cells using microtitration analysis in accordance with the Reed–Muench method (13).

2.6 Immunoblotting

Cell or supernatant samples were harvested and boiled in loading buffer (0.08 M Tris, pH 6.8, with 2.0% SDS, 10% glycerol, 0.1 M dithiothreitol [DTT], and 0.2% bromophenol blue), followed by separation on sodium dodecyl sulphate–polyacrylamide gel electrophoresis and transferred to nitrocellulose membranes using a semi-dry apparatus (Bio-Rad, USA). Membranes were incubated with primary antibodies (anti-EV-D68 VP1 polyclonal antibody [Genetex, GTX132312]; anti- β -actin monoclonal antibody [Sigma, A3853]). Standard alkaline phosphatase-conjugated anti-rabbit IgG or anti-mouse IgG secondary antibodies (goat anti-rabbit IgG [Jackson ImmunoResearch Laboratories, code:115-005-045]; goat anti-mouse IgG [Jackson ImmunoResearch Laboratories, code: 115-055-062]) were then used. The membranes were stained with 5-bromo-4-chloro-3-indolyl phosphate and nitrotetrazolium blue chloride (Sigma-Aldrich) and visualized for band quantification.

2.7 Enzyme-linked immunosorbent assay

The quantification of interferon- α (IFN- α) or interferon- β (IFN- β) in the cell culture media was detected by ELISA kit (Shanghai Jianglai Industrial Limited by Share Ltd., JL12191, JL19215, China) according to the manufacturer's instructions. A monoclonal antibody specific for IFN- α or IFN- β has been coated onto the wells of the micotiter strips (96-well ELISA plate) provided. Samples, including standards of known IFN- α or IFN- β concentrations, control specimens or unknowns were pipetted in triplicate into these wells. During the first incubation, the standards or samples and a biotinylated monoclonal antibody specific for IFN- α or IFN- β were simultaneously incubated. After washing, the enzyme Streptavidin-HRP, that binds the biotinylated antibody was added, incubated and washed. A TMB substrate solution was added which acted on the bound enzyme to induce a colored reaction product. The intensity of this colored product was directly proportional to the concentration of IFN- α or IFN- β present in the samples. The absorbance value was measured at 450 nm wavelength using a BioTek ELISA Reader (BioTek Instruments, Inc., USA).

2.8 Lentivirus production and gene silencing

HEK293T cells were co-transfected with plasmids sh-IRF3-pLKO.1 or non-targeting shRNA as shcontrol plus pRSV-Rev (12253), pMDLg/pRRE (12251), and pCMV-VSV-G (8454) (Addgene) with PEI. 48h post transfection, supernatants containing packaged lentivirus were harvested and cleared by centrifugation. Then A549 cells were transduced with the lentiviruses for 2 days. Puromycin (1.5 μ g/ml) was then added into the culture medium to screen for stable cell lines in which IRF3 or control was shut down. Knockdown efficiency of IRF3 gene was examined by immunoblotting.

2.9 Statistical analysis

All statistical analyses were performed using GraphPad Prism software (version 8.0). Statistical analyses were performed using one-way analysis of variance (ANOVA). Statistical significance was set at $P < 0.05$.

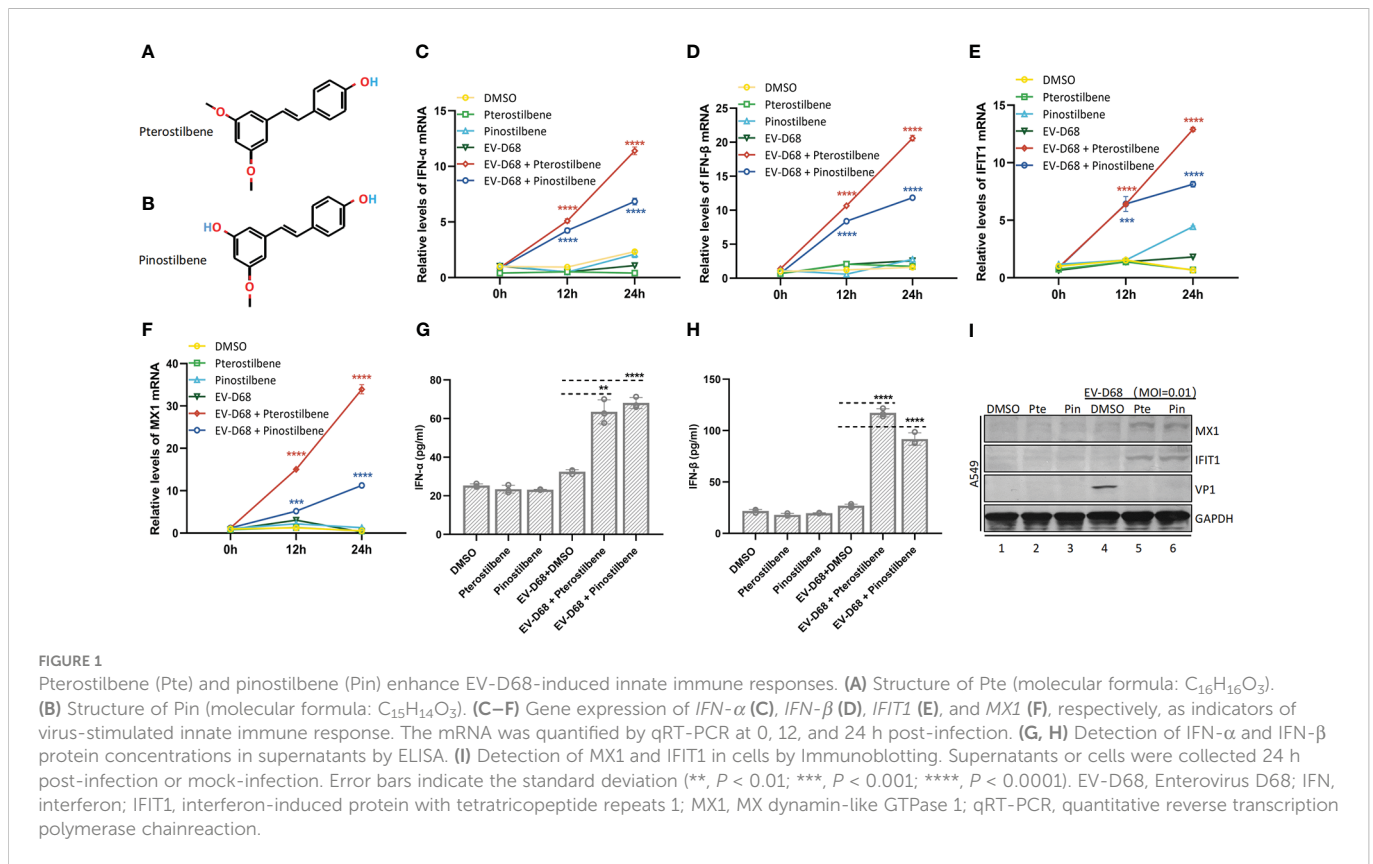
3 Results

3.1 Pte facilitates innate immune activation during EV-D68 infection

Pterostilbene (trans-3,5-dimethoxy-4-hydroxystilbene) and pinostilbene (3,4-dihydroxy-5-methoxy-trans-stilbene), naturally occurring methylated derivatives of resveratrol (3,5,4-trihydroxystilbene), exert anti-inflammatory and immunomodulatory effects (Figures 1A, B). First, we investigated the effects of Pte and Pin on the host innate immune response to EV-D68 infection. A549 human lung adenocarcinoma cells were treated with 25 μ M Pte or Pin in the presence or absence of EV-D68 (MOI = 0.01). Endogenous mRNA levels of the IFN- α , IFN- β and interferon-stimulated genes, *IFIT1* and *MX1*, were measured at 0, 12, and 24 h post-infection (Figures 1C–F). The protein expression of IFN- α , IFN- β , *MX1* and *IFIT1* in supernatant or cell was also detected (Figures 1G–I). The data indicated that single treatment with Pte or Pin during EV-D68 infection did not influence intrinsic innate immune status, as there were no observable changes in the expression of IFN- α , IFN- β , *IFIT1*, or *MX1* (Figures 1C–I). However, a dramatic increase in IFN- α and IFN- β expression was detected in EV-D68-infected cells in the presence of Pte or Pin in a time-dependent manner (Figures 1C, D, G, H). The changes in interferon-stimulated gene (ISG) expression levels further supported that Pte or its derivative, Pin, could enhance the innate immune response to EV-D68 infection, even though EV-D68 infection itself did not trigger immune activation (Figures 1E, F, I).

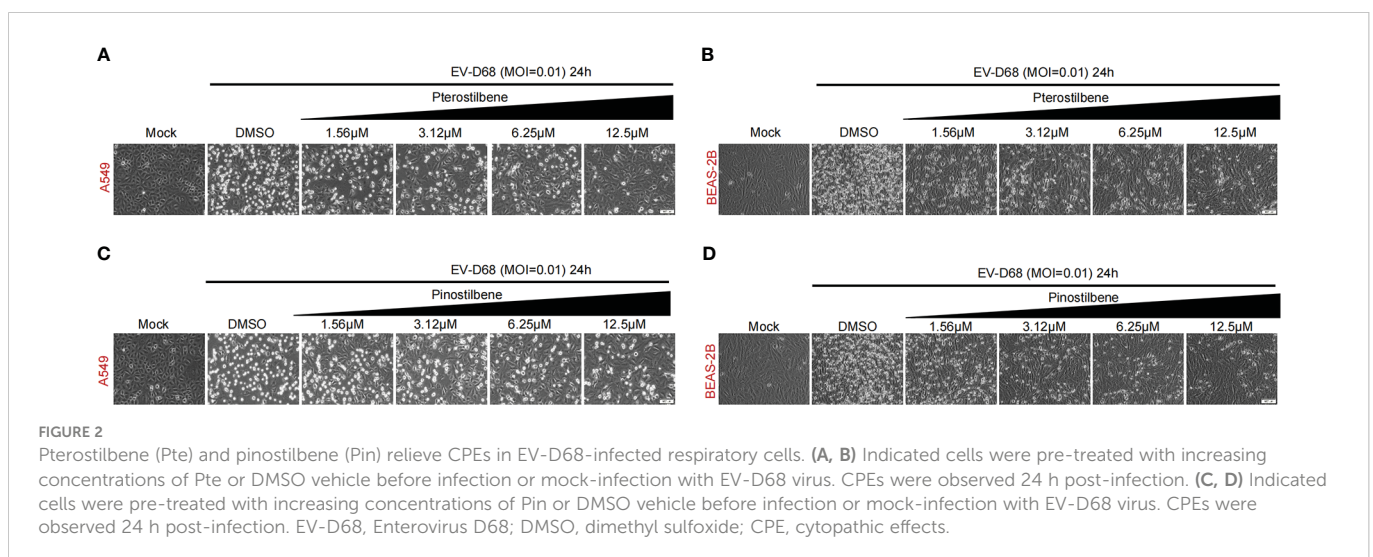
3.2 Pte and Pin inhibit EV-D68 replication

Research has demonstrated that type-I IFN potently inhibits EV-D68 infection (14). Therefore, we investigated the anti-EV-D68 activities of Pte and Pin. In vehicle-treated respiratory A549 and BEAS-2B cells, EV-D68 infection triggered clear CPEs. However, Pte and Pin treatment relieved virus-associated CPEs in a dose-dependent manner (Figure 2).



We also treated A549 cells with increasing concentrations of Pte or Pin (1.56, 3.125, 6.25, 12.5, and 25 μ M), followed by challenge with EV-D68 prototype Fermon virus (MOI = 0.01). Pte and Pin treatment substantially decreased the viral titers of EV-D68 progeny virions compared to those of vehicle DMSO treatment (Figures 3A, B). Similar results were also obtained in BEAS-2B cells (Figures 3C, D). Furthermore, qRT-PCR data supported our conclusion by confirming that Pte and Pin suppressed EV-D68 RNA replication in A549 (Figures 3E, I) and BEAS-2B (Figures 3F, J) cells. The EC_{50} values of Pte against EV-D68 infection were 2.015 μ M (A549 cells) and 4.997 μ M (BEAS-2B

cells). Pin showed more efficient anti-EV-D68 activity, with EC_{50} values of 1.336 μ M (A549 cells) and 2.696 μ M (BEAS-2B cells). Furthermore, the cell viability assay showed no substantial changes in cytotoxicity in cells treated with concentrations as high as 100 μ M Pte or Pin (Figures 3G–L). The CC_{50} values of Pte were 246.7 μ M (A549 cells) and 312.8 μ M (BEAS-2B cells). For Pin, the CC_{50} values were 177.8 μ M (A549 cells) and 337.8 μ M (BEAS-2B cells). Selection index (SI) of antiviral effect = CC_{50}/EC_{50} . SI value of Pte in A549 cells was 122.4; SI value of Pin in A549 cells was 133.1; SI value of Pte in BEAS-2B cells was 62.6; SI value of Pin in BEAS-2B cells was 125.3.



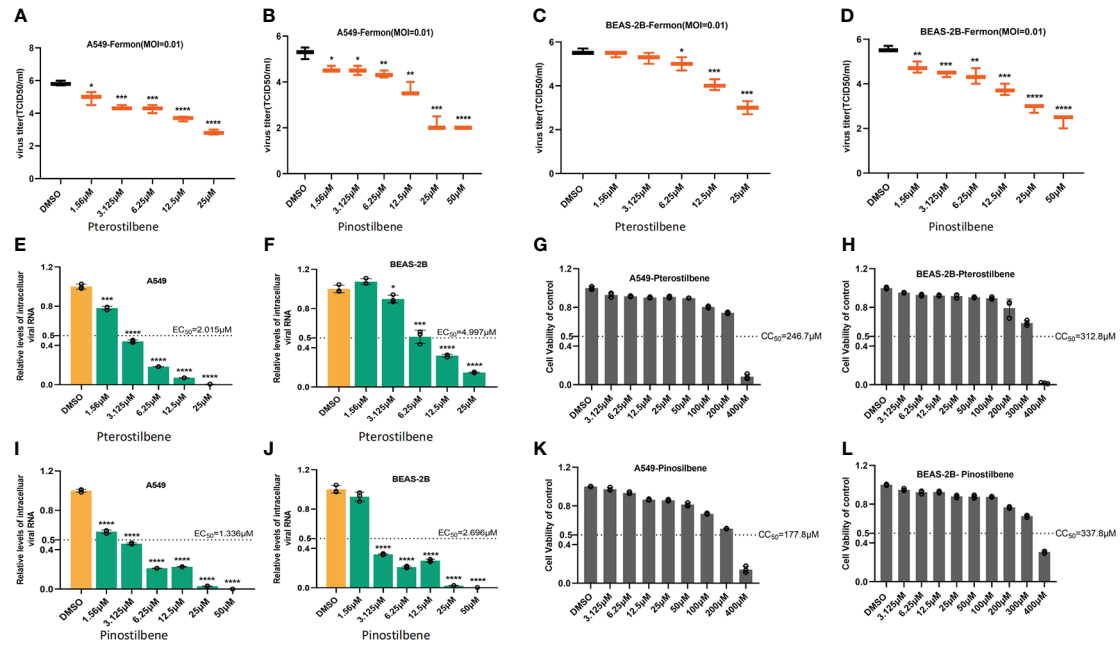


FIGURE 3 Pterostilbene (Pte) and pinostilbene (Pin) inhibit EV-D68 replication. (A–D) Determination of progeny virion production. Supernatants were collected 24 h post-infection and viral titers were determined by standard plaque assay. (E–J) qRT-PCR assessment of EV-D68 RNA replication. (G–L) Cell viability assay. Cellular toxicity was evaluated by CCK-8 assay and is expressed as the percentage relative to DMSO vehicle-treated control cells. Experiments were performed in triplicate. Error bars indicate the standard deviation (*, $P < 0.05$; **, $P < 0.01$; ***, $P < 0.001$; ****, $P < 0.0001$). EV-D68, Enterovirus D68; DMSO, dimethyl sulfoxide; qRT-PCR, quantitative reverse transcription polymerase chain reaction.

3.3 Pte and Pin do not influence EV-D68 entry into cells

Next, we investigated the effects of Pte and Pin on EV-D68 entry into host cells. Viral attachment and entry experiments were performed in the presence of 25 μM Pte, 25 μM Pin, or DMSO. Viral attachment (at 4 $^{\circ}\text{C}$) and entry (at 37 $^{\circ}\text{C}$) were assessed using the quantification of intracellular EV-D68 RNA 2 h post-infection. Repeated experiments confirmed that neither Pte nor Pin treatment obviously disrupted the attachment of EV-D68 to A549 (Figures 4A,

C) or BEAS-2B cells (Figures 4B, D), although there were slight statistical differences seen in Figures 4A–C. Therefore, Pte/Pin inhibited EV-D68 infection during the post-entry step.

3.4 Pte and Pin inhibit viral RNA replication and VP1 synthesis

We next sought to determine the part of the EV-D68 life cycle after entry that was inhibited by Pte and Pin treatment. We analyzed

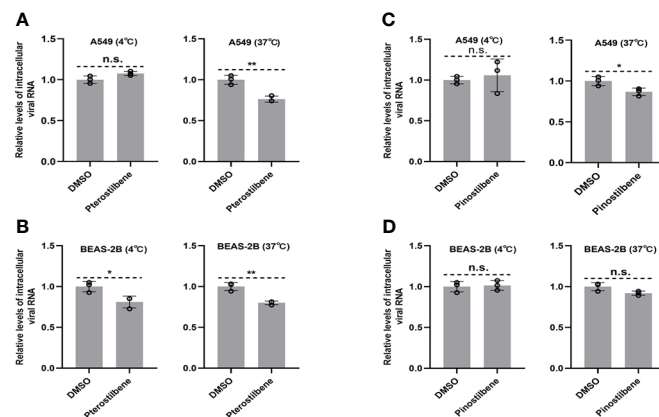


FIGURE 4 Pterostilbene (Pte) and pinostilbene (Pin) do not influence EV-D68 attachment or entry into cells. (A–D) Cells were treated with Pte, Pin, or DMSO vehicle in 12-well plates under standard conditions. Cells were incubated at 4 $^{\circ}\text{C}$ or 37 $^{\circ}\text{C}$ for 30 min before infection and then incubated with EV-D68 viruses for 2 h. The qRT-PCR was performed to quantify viral RNA. EV-D68, Enterovirus D68; DMSO, dimethyl sulfoxide; qRT-PCR, quantitative reverse transcription polymerase chain reaction. Error bars indicate the standard deviation (n.s., no significance, *, $P < 0.05$; **, $P < 0.01$).

EV-D68 growth curves during infection of A549 (MOI = 0.01) and BEAS-2B cells (MOI = 0.01) in the presence of 25 μ M Pte, 25 μ M Pin, or 0.1% DMSO (Figures 5A–D). Viral RNA was quantified at the indicated times after viral infection using qRT-PCR. We noted that Pte and Pin treatment substantially decreased EV-D68 RNA compared to that in the vehicle control at 2 h post-infection (Figures 5A–D). Consistent with these results, we observed a substantial reduction in EV-D68 VP1 protein accumulation in the intracellular portion and supernatant of Pte/Pin-treated cells compared to that of vehicle-treated cells (Figures 5E, F). Hence, treatment with Pte and Pin serves to impede the early stages of EV-D68 infection.

3.5 Pte and Pin suppress isolated circulating strains of EV-D68

Accumulating evidence has demonstrated distinct features between the EV-D68 prototype virus and circulating strains (15). We measured the broad-spectrum activity of Pte and Pin against primary EV-D68 isolates (US/MO/14-18947 [MO] and US/KY/14-18953 [KY]). Similar to the inhibition of EV-D68 prototype Fermon, Pte and Pin treatment substantially decreased the viral titers of the MO (Figures 6A–D) and KY strains (Figures 6E–H) compared to the vehicle control treatment in A549 and BEAS-2B cells. In summary, Pte and its derivative, Pin, exert broad antiviral effects against both the prototype and circulating EV-D68 viruses.

3.6 Pte and Pin mediate innate immune activation through the IRF3 signaling pathway

We further proved that Pte and Pin activate innate immunity through the IRF3 signaling pathway. Synthesis of viral protein VP1 was significantly attenuated in A549-shIRF3 cell lines (Gene knock-down efficiency validation: Figure 7A) in the presence of Pte (25 μ M) or Pin (25 μ M) (Figure 7B). It suggested that Pte and Pin mediated innate immune activation through the IRF3 signaling pathway and achieved antiviral effects. In addition, Pte and Pin could enhance the innate immune activation effect by the RNA virus mimic Poly I:C (Figures 7C–F). This indicated that Pte and Pin may play a role in the interplay between viral RNA replication and activation of the host immune system.

4 Discussion

During the recent coronavirus pandemic, the transmission of other respiratory pathogens worldwide, including EV-D68, dramatically decreased. However, by 2022, several EV-D68 cases have been reported, which may be due to the gradual recovery of social activities (16). Recent research advances in EV-D68 pathogenesis further support that EV-D68 is a neurotropic virus, and its infection is associated with a higher risk of acute flaccid myelitis (17–19). Thus, there is an urgent need to identify safer and more effective anti-EV-D68 drugs. In this study, we showed that

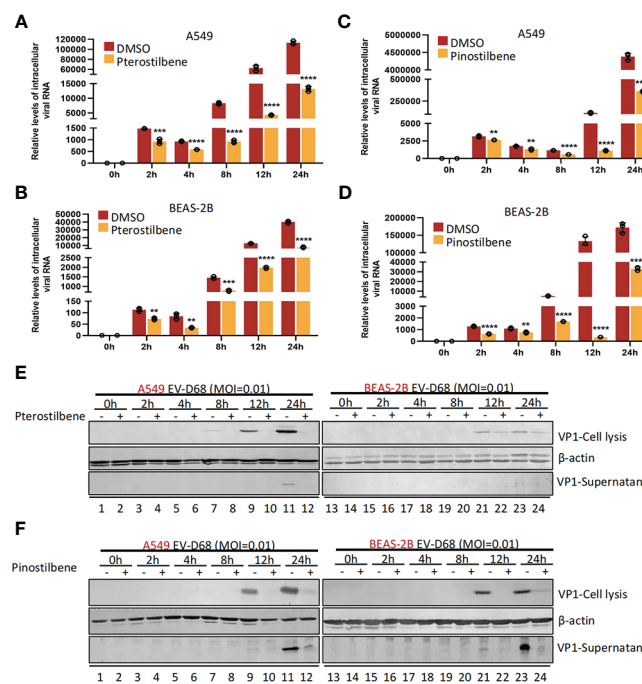


FIGURE 5 Pterostilbene (Pte) and pinostilbene (Pin) suppress EV-D68 RNA replication and VP1 synthesis post viral entry. A549 or BEAS-2B cells were pre-treated with Pte (25 μ M), Pin (25 μ M) or DMSO for 2 h and subsequently infected with EV-D68 at an MOI of 0.01. Cell or supernatant samples were collected at 0, 2, 4, 8, and 12 h post-infection. Relative intracellular viral RNA was detected using qRT-PCR (A–D). Viral structural protein VP1 was measured by immunoblotting (E, F). EV-D68, Enterovirus D68; DMSO, dimethyl sulfoxide; qRT-PCR, quantitative reverse transcription polymerase chain reaction; MOI, multiplicity of infection. Error bars indicate the standard deviation (**, $P < 0.01$; ***, $P < 0.001$; ****, $P < 0.0001$).

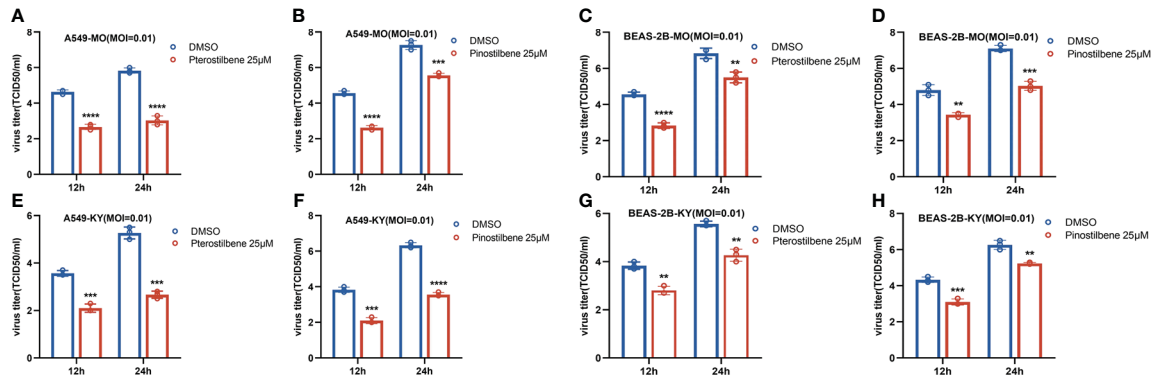


FIGURE 6 Pterostilbene (Pte) and pinostilbene (Pin) inhibit isolated circulating strains of EV-D68. (A–H) A549 or BEAS-2B cells were pre-treated with 25 μ M Pte, or 25 μ M Pin, or DMSO vehicle and then infected with US/MO/14-18947 (MO) or US/KY/14-18953 (KY). Cells were incubated under standard conditions. The titers of progeny virions were determined 12 or 24 h post-infection. The experiment was performed thrice. Error bars indicate the standard deviation (**, $P < 0.01$; ***, $P < 0.001$; ****, $P < 0.0001$). EV-D68, Enterovirus D68; DMSO, dimethyl sulfoxide; MO and KY, isolated EV-D68 circulating strains.

natural products extracted from blueberries (Pte and its derivative, Pin) are potent inhibitors of EV-D68 replication without cytotoxicity at virucidal concentrations.

Host innate immune defense is critical in controlling the invasion of foreign pathogens at an early stage after they enter the body (20). Viruses have evolved diverse strategies to disrupt or evade intracellular innate immune recognition (21, 22). Previous studies have demonstrated that viral proteins encoded by EV-D68, such as 2A, 3C, and 3D, inhibit RIG-I-like receptors, Toll-like receptor-dependent innate immune activation, and IFN production (14, 23–28). Studies have shown that treatment with exogenous IFN robustly blocks EV-D68 infection in cell culture systems (14). Although we did not observe innate immune activation in EV-D68-infected

immortalized cells, EV-D68 infection can initiate cell-type-specific antiviral signaling in human airway epithelial cells and enteroids, which contributes to EV-D68 control (29). Hence, boosting host innate immune recognition and EV-D68 activation is an optimal strategy for drug development. Our data showed that Pte and Pin substantially increased the expression of IFN-I and IFN-stimulated genes in EV-D68-infected cells. Enhanced innate immune activation by Pte/Pin stimulates IFN signaling to mobilize host antiviral factors and clear viral infections. During the preparation of our manuscript, a new study reported that Pte could inhibit influenza virus infection by modulating innate immune responses (30), which also supports our conclusion. Interestingly, we noted that treatment with Pte and Pin did not influence the innate immune status in human respiratory cells

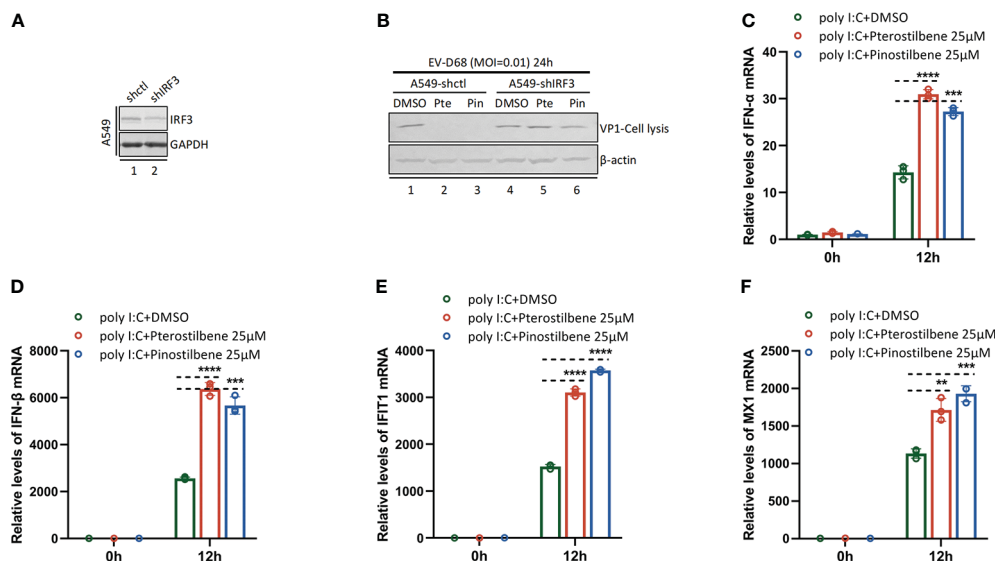


FIGURE 7 Pterostilbene (Pte) and pinostilbene (Pin) mediate innate immune activation through IRF3 signaling pathway. (A) IRF3 gene knock-down efficiency validation by Immunoblotting. (B) A549-shctrl or A549-shIRF3 cells were pre-treated with Pte (25 μ M), Pin (25 μ M) or 0.1% DMSO for 2h and then infected with EV-D68 at an MOI of 0.01. Cells were collected 24 h post-infection. Viral protein VP1 was detected using Immunoblotting. (C–F), A549 cells were pre-treated with Pte, Pin or DMSO for 2h, then transfected with Poly I:C (1 μ g per well). Cells were collected at 0h and 12h post-transfection. Relative intracellular IFN- α , IFN- β , MX1 and IFIT1 mRNA were detected using qRT-PCR. Error bars indicate the standard deviation (**, $P < 0.01$; ***, $P < 0.001$; ****, $P < 0.0001$).

in the absence of EV-D68, which highlights the safety of Pte and Pin for future clinical use.

Recent studies have identified a series of IFN-stimulated genes that maintain anti-enterovirus activities that can block viral replication at different stages of the viral life cycle (31–33). We analyzed the effects of Pte/Pin on the entry of EV-D68 virions and growth curves of EV-D68 RNA replication and VP1 synthesis during infection. Both Pte and Pin dramatically interfere with EV-D68 RNA copy numbers and viral protein accumulation, although no influence was observed on viral invasion of cells. These data suggest that immune activation by Pte/Pin inhibits EV-D68 infection at the post-entry stages of infection. RIG-I-IRF3 is the main upstream signaling pathway that activates interferon. We designed A549 cell lines with stable knockdown of the IRF3 gene, in which even with the presence of Pte or Pin, the anti-EV-D68-effect was significantly impaired, suggesting that Pte or Pin mediates host innate immune activation associated with EV-D68 infection *via* the IRF3 signaling pathway. Poly I:C is an artificial synthetic double-stranded RNA (dsRNA) analog, a molecular pattern associated with viral infection which acts as a potent interferon inducer. Our research confirmed that Pte and Pin could further enhance the activation of interferon by Poly I:C, suggesting that Pte and Pin may have an impact on the interplay between viral RNA replication and host innate immune activation. However, the detailed mechanisms by which Pte/Pin inhibit immune evasion by EV-D68 and promote the blockage of viral replication require further clarification.

Pte exerts a wide range of biological effects on human health, including antioxidative, anti-aging, antitumor, and anti-inflammatory effects (34). An important advantage of Pte over resveratrol is its higher bioavailability. Improved lipophilic properties and oral absorption, higher cellular uptake, and a longer half-life than resveratrol also strengthen its potential for future clinical application (35). Pin is a major metabolite of Pte and plays an important role in the anti-colon cancer effects elicited by orally administered Pte (36). However, the antiviral activities of Pte and Pin, particularly their anti-enteroviral effects, have rarely been investigated. The identification of Pte as a novel anti-EV-D68 agent should accelerate its entry into clinical trials to control the EV-D68 pandemic. The antiviral effects of Pte and Pin against virus infection *in vivo* still need deeper investigation in further studies.

In summary, Pte- and Pin induced time-dependent innate immune activation during EV-D68 infection in human respiratory cells. Concomitantly, the antiviral immune status restricted EV-D68, which failed to complete its life cycle and generate progeny virions. These findings elucidate a novel antiviral strategy to block viral innate immune evasion using natural small-molecule inhibitors. These compounds should be further explored in future clinical investigations.

References

1. Elrick MJ, Pekosz A, Duggal P. Enterovirus D68 molecular and cellular biology and pathogenesis. *J Biol Chem* (2021) 296:100317. doi: 10.1016/j.jbc.2021.100317
2. Liu Y, Sheng J, Baggen J, Meng G, Xiao C, Thibaut HJ, et al. Sialic acid-dependent cell entry of human enterovirus D68. *Nat Commun* (2015) 6:8865. doi: 10.1038/ncomms9865
3. Liu Y, Sheng J, Fokine A, Meng G, Shin WH, Long F, et al. Structure and inhibition of EV-D68, a virus that causes respiratory illness in children. *Science* (2015) 347(6217):71–4. doi: 10.1126/science.1261962
4. Sun J, Hu XY, Yu XF. Current understanding of human enterovirus D68. *Viruses* (2019) 11(6):5. doi: 10.3390/v11060490

Data availability statement

The raw data supporting the conclusions of this article will be made available by the authors, without undue reservation.

Author contributions

QY, HL, and ZL, performed the experiments. WW, QY, JY, ZZ, LZ, and HG analyzed the data. WW, HG, and LZ wrote the paper with help from all authors. W.W. directed the project. All authors contributed to the article and approved the submitted version.

Funding

This work was supported in part by funding from the National Natural Science Foundation of China (32222005, 82172246), the Department of Science and Technology of Jilin Province (No. 20190304033YY), the open project of Key Laboratory of Organ Regeneration and Transplantation, Ministry of Education, the Program for JLU Science and Technology Innovative Research Team (2017TD-08) and Fundamental Research Funds for the Central Universities.

Acknowledgments

We thank Yuanyuan Li and Chuanyan Dai for technical assistance and Editage for editorial assistance.

Conflict of interest

The authors declare that the research was conducted in the absence of any commercial or financial relationships that could be construed as a potential conflict of interest.

Publisher's note

All claims expressed in this article are solely those of the authors and do not necessarily represent those of their affiliated organizations, or those of the publisher, the editors and the reviewers. Any product that may be evaluated in this article, or claim that may be made by its manufacturer, is not guaranteed or endorsed by the publisher.

5. Wei W, Guo H, Chang J, Yu Y, Liu G, Zhang N, et al. ICAM-5/Telencephalin is a functional entry receptor for enterovirus D68. *Cell Host Microbe* (2016) 20(5):631–41. doi: 10.1016/j.chom.2016.09.013
6. Morrey JD, Wang H, Hurst BL, Zukor K, Siddharthan V, Van Wettene AJ, et al. Causation of acute flaccid paralysis by myelitis and myositis in enterovirus-D68 infected mice deficient in interferon $\alpha/\beta/\gamma$ receptor deficient mice. *Viruses* (2018) 10(1):1. doi: 10.3390/v10010033
7. Greninger AL, Naccache SN, Messacar K, Clayton A, Yu G, Somasekar S, et al. A novel outbreak enterovirus D68 strain associated with acute flaccid myelitis cases in the USA (2012–14): A retrospective cohort study. *Lancet Infect Dis* (2015) 15(6):671–82. doi: 10.1016/S1473-3099(15)70093-9
8. Schieble JH, Fox VL, Lennette EH. A probable new human picornavirus associated with respiratory diseases. *Am J Epidemiol.* (1967) 85(2):297–310. doi: 10.1093/oxfordjournals.aje.a120693
9. Midgley CM, Jackson MA, Selvarangan R, Turabelidze G, Obringer E, Johnson D, et al. Severe respiratory illness associated with enterovirus D68 - Missouri and Illinois, 2014. *MMWR Morb Mortal Wkly Rep* (2014) 63(36):798–9. doi: 10.1111/ajtm.13035
10. Nagao K, Jinnouchi T, Kai S, Yanagita T. Pterostilbene, a dimethylated analog of resveratrol, promotes energy metabolism in obese rats. *J Nutr Biochem* (2017) 43:151–5. doi: 10.1016/j.jnutbio.2017.02.009
11. Chen RJ, Kuo HC, Cheng LH, Lee YH, Chang WT, Wang BJ, et al. Apoptotic and nonapoptotic activities of pterostilbene against cancer. *Int J Mol Sci* (2018) 19(1):5. doi: 10.3390/ijms19010287
12. Rossi M, Caruso F, Antonioletti R, Viglianti A, Traversi G, Leone S, et al. Scavenging of hydroxyl radical by resveratrol and related natural stilbenes after hydrogen peroxide attack on DNA. *Chem Biol Interact* (2013) 206(2):175–85. doi: 10.1016/j.cbi.2013.09.013
13. Reed LJ, Muench H. A simple method of estimating fifty per cent endpoints. *Am J Hyg* (1938) 27(3):493. doi: 10.1093/oxfordjournals.aje.a118408
14. Rui Y, Su J, Wang H, Chang J, Wang S, Zheng W, et al. Disruption of MDA5-mediated innate immune responses by the 3C proteins of coxsackievirus A16, coxsackievirus A6, and enterovirus D68. *J Virol* (2017) 91(13):12. doi: 10.1128/JVI.00546-17
15. Baggen J, Thibaut HJ, Staring J, Jae LT, Liu Y, Guo H, et al. Enterovirus D68 receptor requirements unveiled by haploid genetics. *Proc Natl Acad Sci U S A.* (2016) 113(5):1399–404. doi: 10.1073/pnas.1524498113
16. Ma KC, Winn A, Moline HL, Scobie HM, Midgley CM, Kirking HL, et al. Increase in acute respiratory illnesses among children and adolescents associated with rhinoviruses and enteroviruses, including enterovirus D68 - united states, July–September 2022. *MMWR Morb Mortal Wkly Rep* (2022) 71(40):1265–70. doi: 10.15585/mmwr.mm7140e1
17. Helfferich J, de Lange MM, Benschop KS, Jacobs BC, Van Leer-Buter CC, Meijer A, et al. Epidemiology of acute flaccid myelitis in children in the Netherlands, 2014 to 2019. *Euro Surveill* (2022) 27(42):6. doi: 10.2807/1560-7917.ES.2022.27.42.2200157
18. Yea C, Bitnun A, Branson HM, Ciftci-Kavaklioglu B, Rafay MF, Fortin O, et al. Association of outcomes in acute flaccid myelitis with identification of enterovirus at presentation: A Canadian, nationwide, longitudinal study. *Lancet Child Adolesc Health* (2020) 4(11):828–36. doi: 10.1016/S2352-4642(20)30176-0
19. Vogt MR, Wright PF, Hickey WF, De Buysscher T, Boyd KL, Crowe JE Jr. Enterovirus D68 in the anterior horn cells of a child with acute flaccid myelitis. *N Engl J Med* (2022) 386(21):2059–60. doi: 10.1056/NEJMc2118155
20. Kong E, Jabra-Rizk MA. The great escape: Pathogen versus host. *PLoS Pathog* (2015) 11(3):e1004661. doi: 10.1371/journal.ppat.1004661
21. Schulz KS, Mossman KL. Viral evasion strategies in type I IFN signaling - a summary of recent developments. *Front Immunol* (2016) 7:498. doi: 10.3389/fimmu.2016.00498
22. Honda K, Takaoka A, Taniguchi T. Type I interferon [corrected] gene induction by the interferon regulatory factor family of transcription factors. *Immunity* (2006) 25(3):349–60. doi: 10.1016/j.immuni.2006.08.009
23. Yang Z, Zheng H, Li H, Chen Y, Hou D, Fan Q, et al. The expression of IFN- β is suppressed by the viral 3D polymerase via its impact on PGAM5 expression during enterovirus D68 infection. *Virus Res* (2021) 304:198549. doi: 10.1016/j.virusres.2021.198549
24. Xiao H, Li J, Yang X, Li Z, Wang Y, Rui Y, et al. Ectopic expression of TRIM25 restores RIG-I expression and IFN production reduced by multiple enteroviruses 3C(pro). *Virus Sin* (2021) 36(6):1363–74. doi: 10.1007/s12250-021-00410-x
25. Xiang Z, Liu L, Lei X, Zhou Z, He B, Wang J. 3C protease of enterovirus D68 inhibits cellular defense mediated by interferon regulatory factor 7. *J Virol* (2016) 90(3):1613–21. doi: 10.1128/JVI.02395-15
26. Musharrafieh R, Ma C, Zhang J, Hu Y, Diesing JM, Marty MT, et al. Validating enterovirus D68-2A(pro) as an antiviral drug target and the discovery of telaprevir as a potent D68-2A(pro) inhibitor. *J Virol* (2019) 93(7):2. doi: 10.1128/JVI.02221-18
27. Lei X, Xiao X, Wang J. Innate immunity evasion by enteroviruses: Insights into virus-host interaction. *Viruses* (2016) 8(1):5. doi: 10.3390/v8010022
28. Kang J, Pang Z, Zhou Z, Li X, Liu S, Cheng J, et al. Enterovirus D68 protease 2A (pro) targets TRAF3 to subvert host innate immune responses. *J Virol* (2021) 95(3):5. doi: 10.1128/JVI.01856-20
29. Freeman MC, Wells AI, Ciomperlik-Patton J, Myerburg MM, Yang L, Konopka-Anstadt J, et al. Respiratory and intestinal epithelial cells exhibit differential susceptibility and innate immune responses to contemporary EV-D68 isolates. *Elife* (2021) 10:9. doi: 10.7554/eLife.66687.sa2
30. Wu W, Ye Y, Zhong Y, Yan X, Lin J, Qiu J, et al. RNFpterostilbene effectively inhibits influenza A virus infection by promoting the type I interferon production. *Microbes Infect* (2022) 105062:16. doi: 10.1016/j.micinf.2022.105062
31. Zheng B, Zhou X, Tian L, Wang J, Zhang W. IFN- β 1b induces OAS3 to inhibit EV71 via IFN- β 1b/JAK/STAT1 pathway. *Virus Sin* (2022) 37(5):676–84. doi: 10.1016/j.virs.2022.07.013
32. Ida-Hosonuma M, Iwasaki T, Yoshikawa T, Nagata N, Sato Y, Sata T, et al. The alpha/beta interferon response controls tissue tropism and pathogenicity of poliovirus. *J Virol* (2005) 79(7):4460–9. doi: 10.1128/JVI.79.7.4460-4469.2005
33. Schulte BM, Kramer M, Ansems M, Lanke KH, van Doremalen N, Piganelli JD, et al. Phagocytosis of enterovirus-infected pancreatic beta-cells triggers innate immune responses in human dendritic cells. *Diabetes* (2010) 59(5):1182–91. doi: 10.2337/db09-1071
34. Rimando AM, Cuendet M, Desmarchelier C, Mehta RG, Pezzuto JM, Duke SO. Cancer chemopreventive and antioxidant activities of pterostilbene, a naturally occurring analogue of resveratrol. *J Agric Food Chem* (2002) 50(12):3453–7. doi: 10.1021/jf0116855
35. Wang D, Guo H, Yang H, Wang D, Gao P, Wei W. Pterostilbene, an active constituent of blueberries, suppresses proliferation potential of human cholangiocarcinoma via enhancing the autophagic flux. *Front Pharmacol* (2019) 10:1238. doi: 10.3389/fphar.2019.01238
36. Sun Y, Wu X, Cai X, Song M, Zheng J, Pan C, et al. Identification of pinostilbene as a major colonic metabolite of pterostilbene and its inhibitory effects on colon cancer cells. *Mol Nutr Food Res* (2016) 60(9):1924–32. doi: 10.1002/mnfr.201500989